

# Parametric Gain and Conversion Efficiency in Nanophotonic Waveguides With Dispersive Propagation Coefficients and Loss

S. Roy, M. Santagiustina, *Member, IEEE*, A. Willinger, G. Eisenstein, *Fellow, IEEE*, S. Combrié, and A. De Rossi, *Member, IEEE*

**Abstract**—Nanophotonic waveguides can be engineered in order to exhibit slow mode propagation thereby enhancing the nonlinear responses. In such waveguides, loss and nonlinear coefficients are strongly wavelength dependent, a property that must be considered when the signal to pump detuning is large. Exact formulas for the parametric gain and conversion efficiency, accounting for the dispersion of losses and nonlinearity, are derived here. They can be applied to any waveguide presenting such features; in particular they have been calculated for a III-V semiconductor photonic crystal waveguide, where narrow- and broad-band amplification are predicted. The asymmetry of losses causes major asymmetries in the gain and conversion efficiency, which are no longer simply related as in the case of waveguides in which loss do not depend on the wavelength.

**Index Terms**—Optical parametric amplifiers, optical propagation in dispersive media, optical propagation in nonlinear media, optical waveguides, semiconductor waveguides.

## I. INTRODUCTION

LIGHT-MATTER interactions in a photonic crystal waveguide (PhCW) can be highly enhanced in the slow-mode (SM) propagation regime [1]–[4]. In particular, due to the huge increase of nonlinear optical phenomena PhCWs are very promising, compact and reliable devices for the realization on chip of nonlinear processors [5] and sources [6]. Among nonlinear effects four-wave mixing (FWM) has been experimentally demonstrated and theoretically modelled [7]–[12]. Parametric gain has been also measured [13] with a record of about 11 dB for a 1.3-mm PhCW pumped by less than 1-W peak power [14].

The key feature to effectively enable FWM in waveguides is the dispersion profile tailoring, which has a crucial impact on the

parametric gain, as it determines the phase-matching condition. The target is to design PhCWs in which the group index is large, to enhance the effective nonlinear coefficients, but almost constant in wavelength, to limit the group velocity dispersion (GVD). Several of such designs have been developed [15], [16]; here, without loss of generality we will resort to the design presented in [17].

In SM dispersion engineered structures, the Bloch mode field distribution is highly wavelength dependent and this feature has several consequences. It was soon observed, in fact, that mode reshaping impacts losses, in particular those due to scattering [18], which are the dominating ones when material losses are minimal, e.g., for wavelengths corresponding to less than half the semiconductor bandgap, a condition that minimizes both linear and nonlinear losses and that can be achieved in III-V semiconductor by means of a proper choice of the alloy [19]. So, in SM PhCWs, losses depend in a non trivial way on the wavelength [20]. Moreover, the nonlinear coefficients characterizing the nonlinear Kerr interactions, like self-phase modulation (SPM), cross-phase modulation (XPM) and FWM [9], [21] also become dispersive, as highlighted in [22].

When a nonlinear interaction, like for example FWM, occurs among weakly detuned waves the linear and nonlinear dispersion can be neglected because coefficients are nearly the same and averaged loss and nonlinear coefficients can be used [8], [10], [23]. However, when the detuning between the waves is large, like in the case of Raman scattering [24] and of narrowband optical parametric amplification (NBOPA) [25], these differences must be accounted for, because the use of averaged coefficients lead to wrong results.

For a full understanding of the nonlinear dynamics, spatio-temporal simulations are to be used [26], [27]. However, those simulations are time consuming and so the continuous wave approximation is still an irreplaceable tool for waveguide design, in particular if exact formulas can be derived. An exact formula for the parametric gain in presence of losses was derived in [28] for optical fibers, where the wavelength dependence of loss and nonlinear coefficients is absent. A more comprehensive and very detailed account of exact formulas for parametric interactions in optical fibers can be also found in the book by Marhic [29]. In optical fibers, the effects on FWM due to a difference between the signal and idler loss coefficients were studied in [30]; however, only approximate, perturbative solutions were found and the loss difference was artificially induced in the experiments by Brillouin scattering.

Manuscript received August 28, 2013; revised December 9, 2013 and December 28, 2013; accepted January 6, 2014. Date of publication January 8, 2014; date of current version February 3, 2014.

S. Roy is with the Department of Physics, National Institute of Technology, Warangal 506004, India (e-mail: sroy@nitw.ac.in).

M. Santagiustina is with the Department of Information Engineering, University of Padova, 35131 Padova, Italy (e-mail: marco.santagiustina@unipd.it).

A. Willinger and G. Eisenstein are with Department of Electronic Engineering, Technion, Haifa, Israel (e-mail: amnon.willinger@gmail.com; gad@ee.technion.ac.il).

S. Combrié and A. De Rossi are with Thales Research and Technology, Palaiseau, France (e-mail: sylvain.combrie@thalesgroup.com).

Color versions of one or more of the figures in this paper are available online at <http://ieeexplore.ieee.org>.

Digital Object Identifier 10.1109/JLT.2014.2298913

In this paper, we present a detailed calculation and derive exact formulas for the parametric gain and the FWM conversion efficiency valid for waveguides in which both losses and nonlinearity are highly dispersive, so extending the results of [25]. Though the example of calculations will refer to a particular set of III-V semiconductor PhCWs, the results can be actually applied to any guiding structure in which loss and nonlinearity are both dispersive and so the formulas have a broader field of application.

## II. PARAMETRIC GAIN IN WAVEGUIDES WITH DISPERSIVE LOSS AND NONLINEARITY

The interaction among a (degenerate) pump, a signal and an idler wave (at wavelengths  $\lambda_{p,s,i} = 2\pi c_0 / \omega_{p,s,i}$ ) satisfying the degenerate FWM (DFWM) frequency matching condition  $\omega_p - \omega_i = \omega_s - \omega_p = \Delta\omega$ , in a PhCW with dispersive losses and nonlinearity is governed by the following propagation equations for the slowly varying envelopes  $A_l$ , where the pedice  $l$  is respectively  $p$  for the pump,  $s$  for the signal and  $i$  for the idler:

$$\begin{aligned} \frac{dA_p}{dz} &= \left\{ -\frac{\alpha_p}{2} + i\gamma_p |A_p|^2 + 2i [\gamma_{ps} |A_s|^2 + \gamma_{pi} |A_i|^2] \right\} A_p \\ &\quad + 2i\gamma_{Fp} A_p^* A_s A_i \exp(i\Delta\beta z), \\ \frac{dA_s}{dz} &= \left\{ -\frac{\alpha_s}{2} + i\gamma_s |A_s|^2 + 2i [\gamma_{sp} |A_p|^2 + \gamma_{si} |A_i|^2] \right\} A_s \\ &\quad + i\gamma_{Fs} A_p^2 A_i^* \exp(-i\Delta\beta z), \\ \frac{dA_i}{dz} &= \left\{ -\frac{\alpha_i}{2} + i\gamma_i |A_i|^2 + 2i [\gamma_{ip} |A_p|^2 + \gamma_{is} |A_s|^2] \right\} A_i \\ &\quad + i\gamma_{Fi} A_p^2 A_s^* \exp(-i\Delta\beta z). \end{aligned} \quad (1)$$

In (1),  $\alpha_l$  are the power loss coefficients,  $\gamma_l$  the effective SPM nonlinear coefficients,  $\gamma_{lh}$  ( $l \neq h$ ) the XPM effective nonlinear coefficients,  $\gamma_{Fl}$  the effective FWM nonlinear coefficients ( $l, h = p, s, i$ ) and finally  $\Delta\beta = \beta_s + \beta_i - 2\beta_p$  is the linear phase mismatch.

The nonlinear effective coefficients for DFWM have the same definitions as in [9], [22], so they depend on the group indices of the waves involved in the interaction (SM enhancement factor) and on the mode field distribution though normalized overlap integrals. The calculation and wavelength dependence of nonlinear coefficients has been studied in detail in [9], [22]; here we only recall that their estimated value is about  $3 \text{ W}^{-1} \text{ mm}^{-1}$ , large enough to enable on chip nonlinear processing.

In the undepleted pump approximation, i.e. by neglecting all the nonlinear terms that depend on the signal and idler powers in (1), an exact formula of the parametric gain and conversion efficiency for the PhCWs can be derived by extending the results of ref. [29]. The final formulas are given in (9) and (10); their derivation, which follows below, entails several changes of variables and the solution of special equations; so, a reader not interested in all the details can go directly to those equations and the discussion that will follow.

From (1), the solution for the pump wave can be obtained:

$$A_p(z) = \sqrt{P_0} \exp[-\alpha_p z/2 + i\gamma_p P_0 L_p(z)],$$

where  $P_0$  is the input pump power and

$$L_p(z) = \alpha_p^{-1} [1 - \exp(-\alpha_p z)]$$

is the attenuation effective length for the pump. By substituting the expression for the pump wave into the second and third of (1), neglecting the SPM and XPM terms of the signal and the idler, and through a change of variables:

$$\bar{A}_{s,i} = A_{s,i} \exp[\alpha_{s,i} z/2 - i2\gamma_{sp,ip} P_0 L_p(z)]$$

one gets:

$$\frac{d\bar{A}_s}{dz} = F_s(z) \bar{A}_i^*, \quad \frac{d\bar{A}_i}{dz} = F_i(z) \bar{A}_s^* \quad (2)$$

where

$$\begin{aligned} F_{s,i}(z) &= i\gamma_{Fs,Fi} P_0 \exp\{-(\alpha_p \pm \Delta\alpha)z \\ &\quad + i[2\gamma_{pm} P_0 L_p(z) - \Delta\beta z]\}. \end{aligned} \quad (3)$$

The coefficient  $\Delta\alpha = (\alpha_i - \alpha_s)/2$  accounts for the loss dispersion (the plus sign applies for the signal and the minus sign for the idler) and the nonlinear coefficient  $\gamma_{pm} = \gamma_p - \gamma_{sp} - \gamma_{ip}$  sets the strength of the contribution of the nonlinearity to the phase matching condition. From (2)–(3), the effects due to the loss terms can be highlighted: 1) the gain decreases and 2) the phase matching condition depends on the coordinate  $z$  through the effective attenuation length  $L_p(z)$ .

By differentiating (2) with respect to  $z$  and through another change of variables,

$$B_{s,i} = \bar{A}_{s,i} \exp\{1/2[(\alpha_p \pm \Delta\alpha)z - i[2\gamma_{pm} P_0 L_p(z) - \Delta\beta z]]\}$$

equations for  $B_{s,i}$  are obtained:

$$\frac{d^2 B_{s,i}}{dz^2} - g_{s,i}^2(z) B_{s,i} = 0 \quad (4)$$

where  $g_{s,i}^2(z) = P \exp(-2\alpha_p z) + Q_{s,i} \exp(-\alpha_p z) + R_{s,i}$ , with

$$P = (\gamma_{Fs} \gamma_{Fi}^* - |\gamma_{pm}|^2) P_0^2,$$

$$Q_{s,i} = -i(\pm\Delta\alpha + i\Delta\beta) \gamma_{pm} P_0$$

and

$$R_{s,i} = (\alpha_p \pm \Delta\alpha + i\Delta\beta)^2 / 4.$$

where the plus sign applies for the signal equation and the minus sign for the idler equation. In the absence of losses, (4) reduce to the well known formula obtained in the context of optical fibers [29], in which the parametric gain coefficient  $g$  is not a function of  $z$ . Let us highlight that, from the definitions of the parameters  $P, Q_{s,i}$  and  $R_{s,i}$ , one can expect that loss dispersion can make the gain coefficient  $G_s$  and the conversion efficiency  $\eta$  asymmetric with respect to the pump wavelength. In fact moving the signal to be amplified from the Stokes to the anti-Stokes side of the pump wavelength (or viceversa) causes a change of the sign of  $\Delta\alpha$  and so the gain coefficient  $g(z)$  will be different. In practice a change of the sign of the signal to pump detuning  $\Delta\lambda = \lambda_s - \lambda_p$  corresponds to exchanging the roles (and the governing equations) between the signal and the idler. Remarkably, the dispersion of the nonlinear coefficients does not lead to a gain asymmetry; in fact exchanging the signal

and idler coefficients ( $\gamma_{Fs} \leftrightarrow \gamma_{Fi}$ ,  $\gamma_{sp} \leftrightarrow \gamma_{ip}$ ) there is no effect on the values of  $P$  and  $Q_{s,i}$ .

By performing another set of variable changes:

$$\begin{aligned} x &= \exp(-\alpha_p z), & \bar{B}_{s,i} &= x^{1/2} B_{s,i}, \\ y &= y_0 x, & y_0 &= 2P^{1/2}/\alpha_p. \end{aligned}$$

Equation (4) can be cast in the following form:

$$\frac{d^2 \bar{B}_{s,i}}{dy^2} + \left[ -\frac{1}{4} + \frac{k_{s,i}}{y} + \left( \frac{1}{4} - m_{s,i}^2 \right) \frac{1}{y^2} \right] \bar{B}_{s,i} = 0 \quad (5)$$

that is the Whittaker equation of complex parameters

$$k_{s,i} = -Q_{s,i}/(2\alpha_p P^{1/2}) \quad \text{and} \quad m_{s,i} = R_{s,i}^{1/2}/\alpha_p$$

whose solutions are the Whittaker confluent hypergeometric functions  $M_{K,M}(y)$ ,  $W_{K,M}(y)$  ( $K = k_{s,i}$ ,  $M = m_{s,i}$ ) [29], [31].

The general solution of (5) for the signal is

$$\bar{B}_s(y) = U_s M_{k_s, m_s}(y) + V_s W_{k_s, m_s}(y)$$

where  $U_s$ ,  $V_s$  are constants of integration.

For  $z = 0$  (i.e.,  $x = 1, y = y_0$ ) from the previous changes of variables, one gets:

$$\bar{B}_s(y_0) = U_s M_{k_s, m_s}(y_0) + V_s W_{k_s, m_s}(y_0) = A_s(z = 0). \quad (6)$$

To calculate the gain a second relation can be obtained by differentiating the general solution and evaluating the resulting expression for  $y = y_0$ , also considering that  $A_i(z = 0) = 0$ :

$$U_s M'_{k_s, m_s}(y_0) + V_s W'_{k_s, m_s}(y_0) = C A_s(z = 0) \quad (7)$$

where  $M'_{k_s, m_s}(y)$ ,  $W'_{k_s, m_s}(y)$  are the derivatives of the Whittaker confluent hypergeometric functions, that are recursively related to  $M_{k_s, m_s}(y)$ ,  $W_{k_s, m_s}(y)$  [31] and

$$C = \{1 + \alpha_p^{-1} [\iota 2\gamma_{pm} P_0 - (\alpha_p + \Delta\alpha + \iota\Delta\beta)]\}/(2y_0)$$

is a constant.

By solving the linear system of (6) and (7),  $U_s$ ,  $V_s$  are determined and the solution for  $\bar{B}_s$  reads:

$$\begin{aligned} \bar{B}_s(y) &= A_s(z = 0) [\bar{W}_s(y_0)]^{-1} \\ &\times \{ [W'_{k_s, m_s}(y_0) - C W_{k_s, m_s}(y_0)] M_{k_s, m_s}(y) \\ &+ [C M_{k_s, m_s}(y_0) - M'_{k_s, m_s}(y_0)] W_{k_s, m_s}(y) \} \quad (8) \end{aligned}$$

where

$$\bar{W}_s(y_0) = M_{k_s, m_s}(y_0) W'_{k_s, m_s}(y_0) - M'_{k_s, m_s}(y_0) W_{k_s, m_s}(y_0).$$

Finally the signal gain for a PhCW of length  $L$  can be determined:

$$\begin{aligned} G_s(L) &= |A_s(z = L)/A_s(z = 0)|^2 \\ &= \exp(-\alpha_m L) |\bar{W}_s(y_0)|^{-2} \\ &\times \{ [W'_{k_s, m_s}(y_0) - C W_{k_s, m_s}(y_0)] M_{k_s, m_s}(y_L) \\ &+ [C M_{k_s, m_s}(y_0) - M'_{k_s, m_s}(y_0)] W_{k_s, m_s}(y_L) \}^2 \quad (9) \end{aligned}$$

where  $\alpha_m = (\alpha_i + \alpha_s)/2$  and  $y_L = y_0 \exp(-\alpha_p L)$ . With the same assumption and steps, by calculating the solution for the

idler ((5) for  $\bar{B}_i$ ), a formula for the conversion efficiency is obtained:

$$\begin{aligned} \eta &= |A_i(z = L)/A_s(z = 0)|^2 \\ &= \exp(-\alpha_m L) |\bar{W}_i(y_0)|^{-2} \times \{ [\gamma_{Fi} P_0 / \alpha_p y_0] \\ &\times [W'_{k_i, m_i}(y_0) M_{k_i, m_i}(y_L) - M'_{k_i, m_i}(y_0) W_{k_i, m_i}(y_L)] \}^2, \end{aligned} \quad (10)$$

where

$$\bar{W}_i(y_0) = M_{k_i, m_i}(y_0) W'_{k_i, m_i}(y_0) - M'_{k_i, m_i}(y_0) W_{k_i, m_i}(y_0).$$

Note that (9) and (10) cannot be used for lossless waveguides, because  $\alpha_p$  appears at the denominator of several of the constants previously defined. However it has been verified that for negligible, but not zero losses, Equations (9) and (10) yield the same results of lossless waveguides [9].

Similarly, when  $P_0 \rightarrow 0$  then  $y_0 \rightarrow 0$  and (9) cannot be used because the constant  $C$  diverges to infinity. This is not a problem for the conversion efficiency formula, (10), that can be calculated also for  $P_0 \rightarrow 0$  because  $P_0/y_0$  has a finite limit.

### III. CASE STUDY: III-V SEMICONDUCTOR WAVEGUIDES

As mentioned before, dispersion engineered PhCWs for enhancing FWM can be designed in many ways. As an example to test the obtained formulas, we consider the two-dimensional structure that has been proposed in [17]. In particular, the results presented here refer to a membrane PhCW having the air-holes in a triangular lattice with parameters  $a = 484$  nm (crystal period),  $d = 0.25a$  (hole diameter), and  $h = 185$  nm (slab height). The air holes of the innermost row have a diameter  $d_1 = 0.24a$  and are shifted outward by  $0.18a$ . The GVD is tailored by means of a structural modification that consists in a shift of an amount  $T$  of the innermost air-holes rows along the propagation axis but with opposite directions on each side of the PhCW. Here, the translation parameter is set to  $T = 0.08a$ . Such structural shift of air-holes couples an even and an odd mode resulting in a well confined quasi-even mode which nurtures nonlinear effects [9]. The waveguide, of length  $L = 1.3$  mm, was realized in GaInP and the group index and the losses were experimentally measured. Following [20], a fitting relation to determine the propagation loss has been obtained as a function of group index. In particular for the PhCW considered here losses in decibel are given by

$$\alpha(n_g) = [7.897 \tanh(n_g - 20.25) + 0.2998 n_g + 6.319] \text{ dB}.$$

To determine nonlinear coefficients consistent with the losses, the mode field distribution and the group index have been calculated through a full vectorial analysis with the MPB code [32]. In Fig. 1 the calculated group index,  $n_g$ , and the loss fitting function are represented as a function of wavelength, respectively by the blue solid and green dotted line. In Fig. 2 the GVD coefficient  $\beta_2 = d^2 \beta / d\omega^2$  (red curve) and the fourth-order dispersion coefficient  $\beta_4 = d^4 \beta / d\omega^4$  (blue curve) are also plotted as a function of wavelength. The PhCW presents two zero dispersion wavelengths (ZDW,  $\lambda_{01} \simeq 1572$  nm and  $\lambda_{02} \simeq 1578$  nm). For  $\lambda_{01} < \lambda_p < \lambda_{02}$  the GVD and fourth-order dispersion coefficients are respectively positive and negative

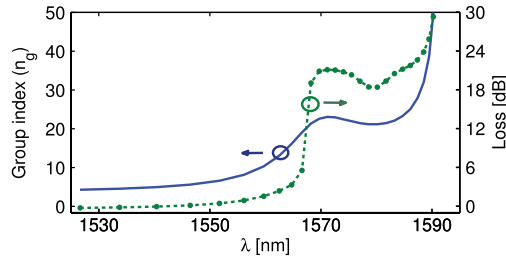


Fig. 1. Group index ( $n_g$ , solid blue curve) and propagation loss (dashed dotted green curve) as a function of wavelength for the case study.

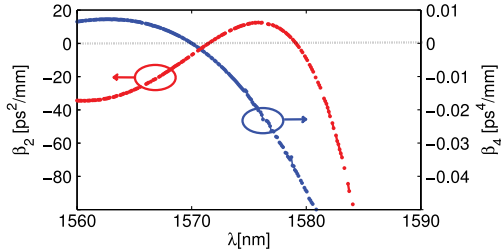


Fig. 2. Second- (red curve) and fourth-order (blue curve) dispersion coefficients as functions of wavelength for the case study.

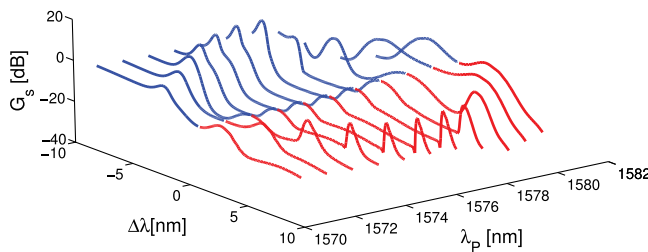


Fig. 3. Parametric gain ( $G_s$ ) for an input pump power of 1 W as a function of signal to pump wavelength detuning and for several values of the pump wavelength in the SM regime.

and so NBOPA can be expected [26]. For  $\lambda_p < \lambda_{01}$  and  $\lambda_p > \lambda_{02}$  where GVD is anomalous, broad band optical parametric amplification (BBOPA) can be expected.

#### IV. NUMERICAL RESULTS AND DISCUSSION

In this section we present the results of the calculation of the parametric gain and the conversion efficiency in the engineered PhCW described in the previous section. For these calculations the pump wavelengths are tuned from 1570 to 1580 nm, i.e., in the flat band of the dispersion curve of Fig. 1, in steps of 1 nm. The gain is presented in Fig. 3 for an input pump power of 1 W, and for different pump wavelengths and several signal to pump detunings  $\Delta\lambda$ . The expected NBOPA regime can be easily recognized and the wavelength of maximum gain can be tuned by modifying the pump wavelength. Noticeably, a BBOPA regime can be also achieved, as expected, for pump wavelengths in the negative GVD regime.

Choosing the same parameters and in the same range of pump wavelengths, we have estimated the corresponding conversion efficiency ( $\eta$ ) using (10). The results are plotted in Fig. 4. In [25] it was shown that the loss dispersion cannot be neglected in the

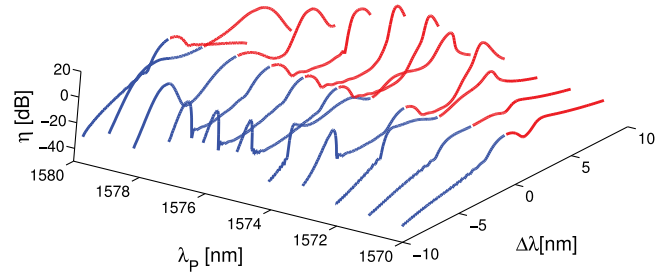


Fig. 4. Conversion efficiency ( $\eta$ ) for an input pump power of 1 W as a function of signal to pump wavelength detuning for several values of the pump wavelength in the SM regime.

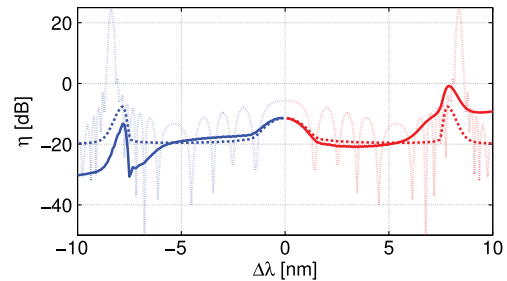


Fig. 5. Comparison of the conversion efficiency as a function of the signal-to-pump detuning ( $P_0 = 1.0$  W,  $L = 1.3$  mm). Dotted curve no losses ( $\alpha_m = 0, \Delta\alpha = 0$ ); solid curve with dispersive losses ( $\alpha_m \neq 0, \Delta\alpha \neq 0$ ); dashed curve with constant losses ( $\alpha_m \neq 0, \Delta\alpha = 0$ ).

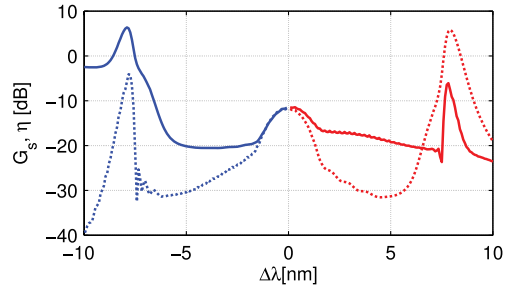


Fig. 6. Parametric gain (solid curve) and the conversion efficiency (dashed curve) for  $\lambda_p = 1575.5$  nm, input pump power 1W.

calculation of the gain for large detunings. The same conclusion must be taken for the conversion too, as shown in Fig. 5 where the predicted conversion efficiency without losses (dotted curve), with constant losses (dashed curve) and with dispersive losses (solid curve) are compared.

To highlight the main results characterizing parametric gain and conversion efficiency in highly linear and nonlinear dispersive waveguide, in Fig. 6 we have plotted both the gain and the conversion efficiency for  $\lambda_p = 1575.5$  nm, a value yielding NBOPA with the maximum pump to signal detuning. Let us first explain how Fig. 6 is to be read, to avoid any misunderstanding, in particular for the conversion efficiency. The abscissa of the plot is the signal to pump wavelength detuning  $\Delta\lambda = \lambda_s - \lambda_p$ . The gain plot represents the ratio between the output and input power for a signal shifted by  $\Delta\lambda$  with respect to the pump wavelength. The conversion efficiency represents the power ratio between the output idler at wavelength  $\lambda_i$  and the input signal

at wavelength  $\lambda_s = \lambda_p + \Delta\lambda$ . Given that the abscissa in Fig. 6 is the signal to pump wavelength detuning, the value of the conversion efficiency at  $\Delta\lambda$  actually refers to the idler which is generated on the other side of the pump wavelength. Note that conversion efficiency is larger than 1 in the best case. This can be explained as follows: the input signal is initially amplified and so the final idler power can be larger than the initial signal amplitude.

The large wavelength asymmetry of gain has been already pointed out in [25]. In fact, a net gain can be achieved only if the signal is placed on the anti-Stoke (blue shifted) side. The reason for this behaviour, as explained in Section II, is that losses (see Fig. 1) are smaller on that side of the pump, while increase on the Stokes (red shifted) side, up to suppress gain completely.

The conversion efficiency is highly asymmetric for the same reason. In particular, the highest conversion is achieved when the signal is placed on the Stokes (red shifted) side, which corresponds to low loss propagation conditions for the idler (that is generated on the anti-Stokes, blue shifted side). This can be also explained by observing the parameters  $Q_{s,i}$ ,  $R_{s,i}$  that define the gain coefficient  $g(z)$  in Section II. For the signal  $+\Delta\alpha$  must be used and the largest gain coefficient is found for  $\Delta\lambda < 0$  that implies  $\Delta\alpha = (\alpha_i - \alpha_s)/2 > 0$  (idler losses are larger than signal losses). For the idler, the gain coefficient is determined by using  $-\Delta\alpha$  in the formulas. So, if the idler is on the anti-Stokes side ( $\lambda_i - \lambda_p < 0 \Rightarrow \Delta\lambda = \lambda_s - \lambda_p > 0$ ) then  $\Delta\alpha < 0$  and since there are two changes of sign in the formulas the highest gain coefficient can be expected.

The conclusion to be taken is that both gain and conversion efficiency spectral behaviours are dominated by losses and loss engineering [20] is a crucial issue, as important as dispersion engineering, to the quest of realizing on chip parametric devices. The amplification/conversion take place in the initial stage of the propagation, where the pump is sufficiently powerful; the amplified/generated wave is then maintained only if losses are minimal. Finally let us remark that for small signal to pump detunings, as already observed, the asymmetry is negligible and thus averaged coefficients and formulas can be effectively used.

The loss induced asymmetry has an additional, remarkable effect that makes this case different from previously studied parametric interactions. In absence of losses the conservation of the number of photons (Manley–Rowe relations) implies that  $P_s(L) - P_i(L) = P_s(0)$ , since  $P_i(0) = 0$ . Therefore  $P_s(L)/P_s(0) - P_i(L)/P_s(0) = G_s - \eta = 1$ . When  $\alpha \neq 0$ , but losses are not function of wavelength, the previous relation becomes:  $\exp(\alpha L)(G_s - \eta) = 1$  [29]. Here, this relation does not hold any longer, even taking into consideration a wavelength dependent loss coefficient. This is due to the fact that the signal and the idler are governed by different equations, as remarked in the discussion about (4). To show this behaviour the parameter  $D = |\exp(\alpha_s L) G_s - \exp(\alpha_i L) \eta|$  has been calculated and it is presented in Fig. 7. Note that  $D \simeq 1$  only when the FWM is not phase-matched, i.e., when gain and conversion efficiency are negligible; however, close to phase-matching conditions  $D$  is very different from 1. This is similar to what occurs when Raman gain, which is also a term causing a Stokes/anti-Stokes asymmetry, is included in the parametric equations [29].

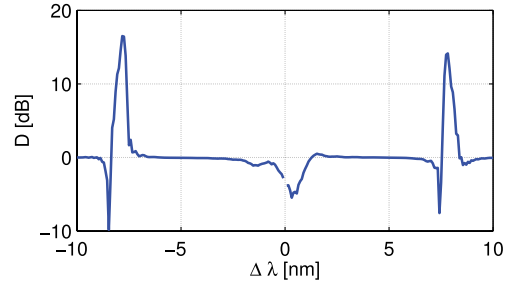


Fig. 7. Parameter  $D = |\exp(\alpha_s L) G_s - \exp(\alpha_i L) \eta|$  as function of wavelength detuning for  $\lambda_p = 1575.5$  nm and for an input pump power of 1W.

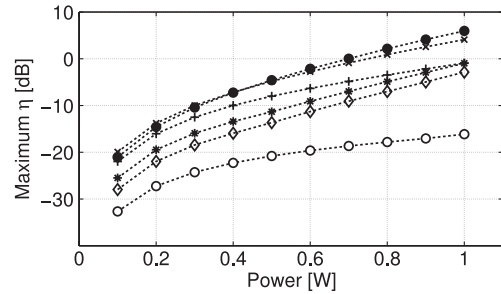


Fig. 8. Maximum conversion efficiency ( $\eta$ ) as function of pump power at different pump wavelengths (empty circle marker,  $\lambda_p = 1570$  nm; plus marker,  $\lambda_p = 1572$  nm; cross marker,  $\lambda_p = 1573$  nm; filled circle marker,  $\lambda_p = 1576$  nm; empty diamond marker,  $\lambda_p = 1577$  nm; asterisk marker,  $\lambda_p = 1579$  nm).

Finally we have studied the power dependence of the conversion efficiency. In Fig. 8, we have presented the maximum conversion efficiency as a function of the input pump power for several pump wavelengths. For  $\lambda_p = 1570$  nm (empty circles), the phase matching condition is satisfied in a high loss regime (see Fig. 1) and therefore, the maximum conversion efficiency is relatively poor. Increasing the pump wavelengths ensures a larger  $\eta$  value. For  $1573 \text{ nm} < \lambda_p < 1576 \text{ nm}$ , the conversion efficiency is larger than 1 if  $P_0 > 0.7W$ .

## V. CONCLUSION

In conclusion, a detailed study of the parametric interactions in photonic crystal waveguides, specially engineered for enhancing degenerate four wave mixing, was carried out. It is fundamental to stress that both the losses and the nonlinearity are highly dispersive in such waveguides, due to the strong wavelength dependence of the Bloch mode field distribution. Therefore, for large values of the signal to pump detuning, standard gain and conversion efficiency formulas, in which only one (average) value of the loss and nonlinear coefficients is used, give uncorrect results. Under the undepleted pump approximation, exact formulas has been derived for determining the parametric gain and the conversion efficiency accounting for the dispersive loss and the dispersive nonlinearity.

The formulas were applied to the case of III–V semiconductor photonic crystal waveguides. For a selected structure the nonlinear overlap integrals that define the nonlinear coefficients have been calculated. The loss coefficient as a function of the wavelength have been derived by an interpolation of the experimental

characterization of the waveguide manufactured with that design. In particular the engineered waveguide presented two zero dispersion wavelengths and a regime of positive GVD in between and it was expected to show both narrow and broad band parametric gain.

In fact, the theoretical and numerical analyses predict that both regimes can be achieved by properly tuning the pump wavelength. The main feature of gain and conversion efficiency is represented by the large spectral asymmetry, solely due to the loss dispersion. This asymmetry also breaks the relation between gain and conversion efficiency which is an intrinsic property of parametric interaction, due to the conservation of the number of photons.

The exact formulas derived here, though applied to a specific photonic crystal waveguide, are actually very general and can find application to any waveguide in which loss and nonlinearity are highly dispersive.

As for the specific results, the narrow band regime is particularly interesting for applications since it can be used as a tool to achieve tunable material slow light, in addition to the structural slowing down effect, and to realized tunable optical parametric oscillators.

#### ACKNOWLEDGMENT

S. Roy acknowledges support from the University of Padova (Iniziative di Cooperazione Universitaria 2013). M. Santagiustina acknowledges support from the University of Padova (project 60A11-5103/13 “Photonic sensors and processors”). A. Willinger and G. Eisenstein acknowledge support from the Israeli Nanotechnology Focal Technology Area on Nano photonics for Detection.

#### REFERENCES

- [1] T. F. Krauss, “Slow light in photonic crystal waveguides,” *J. Phys. D, Appl. Phys.*, vol. 40, no. 9, pp. 2666–2670, May 2007.
- [2] T. Baba, “Slow light in photonic crystals,” *Nature Photon.*, vol. 2, no. 9, pp. 465–473, Aug. 2008.
- [3] J. B. Khurgin and R. S. Tuck, *Slow Light: Science and Applications*. Boca Raton, FL, USA: CRC Press, 2009.
- [4] C. Monat, M. de Sterke, and B. J. Eggleton, “Slow light enhanced nonlinear optics in periodic structures,” *J. Opt.*, vol. 12, 288, no. 10, p. 104003, Oct. 2010.
- [5] B. Corcoran, C. Monat, M. Pelusi, C. Grillet, T. P. White, L. O’Faolain, T. F. Krauss, B. J. Eggleton, and D. J. Moss, “Optical signal processing on a silicon chip at 640Gb/s using slow-light,” *Opt. Exp.*, vol. 18, no. 8, pp. 7770–7781, Apr. 2010.
- [6] L. Zhang, Q. Lin, Y. Yue, Y. Yan, R. G. Beausoleil, and A. E. Willner, “Silicon waveguide with four zero-dispersion wavelengths and its application in on-chip octave-spanning supercontinuum generation,” *Opt. Exp.*, vol. 20, no. 2, pp. 1685–1690, Jan. 2012.
- [7] M. Ebnavi-Heidari, C. Monat, C. Grillet, and M. K. Moravvej-Farshi, “A proposal for enhancing four-wave mixing in slow light engineered photonic crystal waveguides and its application to optical regeneration,” *Opt. Exp.*, vol. 17, no. 20, pp. 18340–18353, Sep. 2009.
- [8] V. Eckhouse, I. Cestier, G. Eisenstein, S. Combié, P. Colman, A. De Rossi, M. Santagiustina, C. G. Someda, and G. Vadalà, “Highly efficient four wave mixing in GaInP photonic crystal waveguides,” *Opt. Lett.*, vol. 35, no. 9, pp. 1440–1442, May 2010.
- [9] M. Santagiustina, C. G. Someda, G. Vadalà, S. Combié, and A. De Rossi, “Theory of slow light enhanced four-wave mixing in photonic crystal waveguides,” *Opt. Exp.*, vol. 18, no. 20, pp. 21024–21029, Sep. 2010.
- [10] C. Monat, M. Ebnavi-Heidari, C. Grillet, B. Corcoran, B. J. Eggleton, T. P. White, L. O’Faolain, J. Li, and T. F. Krauss, “Four-wave mixing in slow light engineered silicon photonic crystal waveguides,” *Opt. Exp.*, vol. 18, no. 22, pp. 22915–22927, Oct. 2010.
- [11] J. Li, L. O’Faolain, I. H. Rey, and T. F. Krauss, “Four-wave mixing in photonic crystal waveguides: Slow light enhancement and limitations,” *Opt. Exp.*, vol. 19, no. 5, pp. 4458–4463, Feb. 2011.
- [12] B. Corcoran, M. D. Pelusi, C. Monat, J. Li, L. O’Faolain, T. F. Krauss, and B. J. Eggleton, “Ultracompact 160 Gbaud all-optical demultiplexing exploiting slow light in an engineered silicon photonic crystal waveguide,” *Opt. Lett.*, vol. 36, no. 9, pp. 1728–1730, May 2011.
- [13] P. Colman, I. Cestier, A. Willinger, S. Combié, G. Lehoucq, G. Eisenstein, and A. De Rossi, “Observation of parametric gain due to four-wave mixing in dispersion engineered GaInP photonic crystal waveguides,” *Opt. Lett.*, vol. 36, no. 14, pp. 2629–2631, Jul. 2011.
- [14] I. Cestier, S. Combié, S. Xavier, G. Lehoucq, A. D. Rossi, and G. Eisenstein, “Chip-scale parametric amplifier with 11-db gain at 1550 nm based on a slow-light GaInP photonic crystal waveguide,” *Opt. Lett.*, vol. 37, no. 9, pp. 3996–3998, Oct. 2012.
- [15] L. H. Frandsen, A. V. Lavrinenco, J. Fage-Pedersen, and P. I. Borel, “Photonic crystal waveguides with semi-slow light and tailored dispersion properties,” *Opt. Exp.*, vol. 14, no. 20, pp. 9444–9450, Oct. 2006.
- [16] J. Li, T. P. White, L. O’Faolain, A. Gomez-Iglesias, and T. F. Krauss, “Systematic design of flat band slow light in photonic crystal waveguides,” *Opt. Expr.*, vol. 16, no. 9, pp. 6227–6232, Apr. 2008.
- [17] P. Colman, S. Combié, G. Lehoucq, and A. De Rossi, “Control of dispersion in photonic crystal waveguides using group symmetry theory,” *Opt. Exp.*, vol. 20, no. 12, pp. 13108–13114, Jun. 2012.
- [18] M. Patterson, S. Hughes, S. Schulz, D. M. Beggs, T. P. White, L. O’Faolain, and T. F. Krauss, “Disorder-induced incoherent scattering losses in photonic crystal waveguides: Bloch mode reshaping, multiple scattering, and breakdown of the Beer–Lambert law,” *Phys. Rev. B*, vol. 80, no. 19, pp. 195305–195310, Nov. 2009.
- [19] S. Combié, Q. Vy Tran, C. Husko, P. Colman, and A. De Rossi, “High quality GaInP nonlinear photonic crystals with minimized nonlinear absorption,” *Appl. Phys. Lett.*, vol. 95, no. 22, pp. 221108–221110, Nov. 2009.
- [20] L. O’Faolain, S. A. Schulz, D. M. Beggs, T. P. White, M. Spasenović, L. Kuipers, F. Morichetti, A. Melloni, S. Mazoyer, J. P. Hugonin, P. Lalanne, and T. F. Krauss, “Loss engineered slow light waveguides,” *Opt. Exp.*, vol. 18, no. 26, pp. 27627–27638, Dec. 2010.
- [21] N. C. Panoiu, J. F. McMillan, and C. W. Wong, “Theoretical analysis of pulse dynamics in silicon photonic crystal wire waveguides,” *IEEE J. Sel. Top. Quantum Electron.*, vol. 16, no. 1, p. 257266, Jan./Feb. 2010.
- [22] S. Roy, M. Santagiustina, P. Colman, S. Combié, and A. De Rossi, “Modeling the dispersion of the nonlinearity in slow mode photonic crystal waveguide,” *IEEE Photon. J.*, vol. 4, no. 1, pp. 224–233, Feb. 2012.
- [23] A. Melloni, F. Morichetti, and M. Martinelli, “Four-wave mixing and wavelength conversion in coupled-resonator optical waveguide,” *J. Opt. Soc. Am. B*, vol. 25, no. 12, pp. C87–C97, Dec. 2008.
- [24] I. H. Rey, Y. Lefevre, S. A. Schulz, N. Vermeulen, and T. F. Krauss, “Scaling of Raman amplification in realistic slowlight photonic crystal waveguides,” *Phys. Rev. B, Condens. Matter Mater. Phys.*, vol. 84, no. 3, p. 035306, Jul. 2011.
- [25] S. Roy, A. Willinger, S. Combié, A. D. Rossi, G. Eisenstein, and M. Santagiustina, “Narrowband optical parametric gain in slow mode engineered GaInP photonic crystal waveguides,” *Opt. Lett.*, vol. 37, no. 14, p. 29192921, Jul. 2012.
- [26] A. Willinger, S. Roy, M. Santagiustina, S. Combié, A. D. Rossi, I. Cestier, and G. Eisenstein, “Parametric gain in dispersion engineered photonic crystal waveguides,” *Opt. Exp.*, vol. 21, no. 4, p. 49955004, Feb. 2013.
- [27] A. Willinger, S. Roy, M. Santagiustina, S. Combié, A. D. Rossi, I. Cestier, and G. Eisenstein, “Dual-pump parametric amplification in dispersion engineered photonic crystal waveguides,” *Opt. Exp.*, vol. 21, no. 9, pp. 10440–10453, May 2013.
- [28] M. Karlsson, “Modulational instability in lossy optical fibers,” *J. Opt. Soc. Amer. B*, vol. 12, no. 11, pp. 2071–2077, Nov. 1995.
- [29] M. E. Marhic, *Optical Parametric Amplifiers, Oscillators, and Related Devices*. Cambridge, U.K.: Cambridge Univ. Press, 2008.
- [30] T. Tanemura, Y. Ozeki, and K. Kikuchi, “Modulational instability and parametric amplification induced by loss dispersion in optical fibers,” *Phys. Rev. Lett.*, vol. 93, no. 16, pp. 163902–163905, Oct. 2004.
- [31] M. Abramowitz and I. A. Stegun, *Handbook of Mathematical Functions*. New York, NY, USA: Dover, 1972.
- [32] J. D. Joannopoulos (2008, Feb.). [Online]. Available: <http://ab-initio.mit.edu/photons/>

Authors’ biographies not available at the time of publication.